Journal of Statistical Physics, Vol. 56, Nos. 3/4, 1989

The Moment Method for Boundary Layer Problems in Brownian Motion Theory

M. E. Widder[1] and U. M. Titulaer[1]

Received October 3, 1988; final February 23, 1989

We apply Grad's moment method, with Hermite moments and Marshak-type boundary conditions, to several boundary layer problems for the Klein–Kramers equation, the kinetic equation for noninteracting Brownian particles, and study its convergence properties as the number of moments is increased. The errors in various quantities of physical interest decrease asymptotically as inverse powers of this number; the exponent is roughly three times as large as in an earlier variational method, based on an expansion in the exact boundary layer eigenfunctions. For the case of a fully absorbing wall (the Milne problem) we obtain full agreement with the recent exact solution of Marshall and Watson; the relevant slip coefficient, the Milne length, is reproduced with an accuracy better than 10^{-6}. We also consider partially absorbing walls, with specular or diffuse reflection of nonabsorbed particles. In the latter case we allow for a temperature difference between the wall and the medium in which the particles move. There is no *a priori* reason why our method should work only for Brownian dynamics; one may hope to extend it to a broad class of linear transport equations. As a first test, we looked at the Milne problem for the BGK equation. In spite of the completely different analytic structure of the boundary layer eigenfunctions, the agreement with the exact solution is almost as good as for the Klein–Kramers equation.

KEY WORDS: Boundary layers; Brownian motion; moment method; Milne problem; albedo problem; BGK equation.

1. INTRODUCTION AND PREVIEW

A system of particles described by a kinetic equation often relaxes rapidly toward a local equilibrium state; its further evolution is then governed by macroscopic hydrodynamic equations. In the hydrodynamic stage the solution of the kinetic equation is of the so-called normal, or

[1] Institut für theoretische Physik, Johannes Kepler Universität Linz, A-4040 Linz, Austria.

0022-4715/89/0800-0471$06.00/0

Chapman–Enskog, type, and the hydrodynamic equations can be derived from the kinetic one by means of the Chapman–Enskog algorithm.[1,2] Complications arise when the boundary conditions for the kinetic equation are incompatible with a Chapman–Enskog form for the solution. This may be the case when the wall absorbs certain types of particles, or when different parts of the wall are kept at different temperatures or velocities. In such cases *kinetic boundary layers* (with a thickness of the order of a mean free path, or of a corresponding characteristic length of the system) develop near the wall; to analyze these layers one has to go back to the underlying kinetic equation. The breakdown of the Chapman–Enskog procedure near the wall implies that the procedure cannot be used to derive the *boundary conditions* to be used with the hydrodynamic equation; these can be derived only from the structure of the kinetic boundary layer. (An example is given at the end of Section 3; comments on earlier work are given in Section 6.)

Thus far there are two exactly solved types of problem involving a kinetic boundary layer. Both concern stationary nonequilibrium solutions of *linear* kinetic equations of the type

$$\frac{\partial P(\mathbf{u}, \mathbf{r}, t)}{\partial t} = -\mathbf{u} \cdot \frac{\partial}{\partial \mathbf{r}} P(\mathbf{u}, \mathbf{r}, t) + \mathscr{C} P(\mathbf{u}, \mathbf{r}, t) \tag{1.1}$$

in a one-dimensional (half-space or slab) geometry; the function $P(\mathbf{u}, \mathbf{r}, t)$ is the joint probability distribution for velocity and position of the particles, and $\mathscr{C}$ is a linear collision operator acting on $\mathbf{u}$ only. The first, and oldest, exactly solved case is for $\mathscr{C}$ of BGK type,

$$\mathscr{C} P = -\gamma [1 - \mathscr{P}] P \tag{1.2}$$

with γ a relaxation rate and $\mathscr{P}$ the projection operator on the local equilibrium state (or states, when there is more than one conserved quantity). A survey of solved cases of this type, and of the available solution techniques, can be found in ref. 2. Recently, Marshall and Watson[3,4] found a second exact solution, namely for the Klein–Kramers[5,6] case

$$\mathscr{C} P = \gamma \frac{\partial}{\partial \mathbf{u}} \cdot \left[\mathbf{u} + \frac{1}{m\beta} \frac{\partial}{\partial \mathbf{u}} \right] P \tag{1.3}$$

With this substitution (1.1) becomes the kinetic equation for noninteracting Brownian particles of mass m and friction coefficient γ in a medium with temperature $T = (k\beta)^{-1}$.

Unfortunately, the exact solutions, especially for the case (1.3), are analytically quite involved, and the extraction of specific results requires a fair amount of additional numerical effort. Perhaps more importantly, the

methods of solution are not easily extendible to different forms of $\mathscr{C}$ [though Marshall and Watson were able to treat the case of a constant external field,[3] for which $\mathbf{u}$ is replaced by $\mathbf{u}-\mathbf{g}/\gamma$ in (1.3)]. On the other hand, surprisingly accurate approximations to the exact solution (then still unknown) were obtained, in particular by Waldenstrøm *et al.*,[7] using a simple adaptation of Grad's[8] truncated set of moment equations [derived from (1.1) in a manner to be described more fully in Section 2] with boundary conditions of Marshak type.[9] This method does not depend too crucially on the precise structure of $\mathscr{C}$, and it is extendible without too much extra effort[10,11] to higher-dimensional cases, especially to highly symmetric ones. We therefore decided to explore the potential of this moment method, and especially its rate of convergence toward the exact solution as the order of truncation is increased. The convergence question is of some interest, since an earlier, apparently more systematic approximation scheme[12] exhibits an extremely slow rate of convergence.

In Section 2 we explain our method and apply it to the classical, stationary Milne problem, i.e., we solve (1.1) with $\mathscr{C}$ given by (1.3) with a plane wall (at $x=0$) that absorbs all Brownian particles that hit it; mathematically, this means that the solution $P_M(\mathbf{u}, \mathbf{r})$ must obey

$$P_M(\mathbf{u}; 0, y, z)=0 \qquad \text{for} \quad u_x>0 \tag{1.4}$$

For $x\to\infty$ the solution is required to approach a Chapman–Enskog solution with a constant current, normalized to unity, flowing toward the boundary. The boundary conditions ensure that the solution has the form

$$P_M(\mathbf{u}, \mathbf{r})=p_M(u_x, x)\frac{m\beta}{2\pi}\exp[-\tfrac{1}{2}m\beta(u_y^2+u_z^2)] \tag{1.5}$$

The N-moment approximations $p_M^N(u_x, x)$ converge toward the exact solution, but in a highly nonuniform way. Good convergence is obtained for the density profile

$$n_M(x)=\int du_x\, p_M(u_x, x) \tag{1.6}$$

The approximants $n_M^N(x)$ for high enough N can be fitted with the empirical formula[12]

$$a^N=a^\infty+bN^{-\delta} \tag{1.7}$$

The convergence exponents are about three times as large as in the earlier, variational scheme of ref. 12, and the extrapolated values $n_M^\infty(x)$ agree with

the exact values, with a discrepancy smaller than the error in $n_M^{\infty}(x)$ caused by numerical roundoff. Roundoff errors at present preclude extending the calculations beyond $N=25$, but this suffices to obtain, e.g., the Milne length x_M, defined by

$$n_M(x) \simeq m\beta\gamma(x + x_M) \qquad \text{for} \quad x \to \infty \tag{1.8}$$

to six significant figures. The quantity x_M is of special interest since it enters into the effective boundary condition for the diffusion equation, which is the hydrodynamic equation derived from the Klein–Kramers equation.

In Sections 3–5 we apply our method to some cases for which the exact solution has not yet been evaluated. In Section 3 we consider the case of a partially reflecting wall, characterized by the boundary condition

$$p_{Mr}(u_x, x) = rp_{Mr}(-u_x, x) \qquad \text{for} \quad u_x > 0 \tag{1.9}$$

with $0 < r < 1$. In Section 4 we consider the albedo problem, i.e., the case that particles are injected into the system at $x=0$ with a prescribed velocity distribution $g(\mathbf{u})$:

$$P_g(\mathbf{u}; 0, y, z) = g(\mathbf{u}) \qquad \text{for} \quad u_x > 0 \tag{1.10}$$

with the additional condition that $n_g(x) = \int d\mathbf{u}\, P_g(\mathbf{u}, x)$ goes to a constant for $x \to \infty$ (no sources or sinks at infinity). The problem can be decomposed into a set of decoupled problems of the type considered in Section 2 by expanding both $g(\mathbf{u})$ and $P_g(\mathbf{u}, x)$ in a complete set of functions $\chi_l(u_y, u_z)$. We confine ourselves to the case that $g(\mathbf{u})$, and hence $P_g(\mathbf{u}, x)$ and the χ_l, depend on u_y and u_z only via $u_t = (u_y^2 + u_z^2)^{1/2}$. Explicit results are given for the case

$$g(\mathbf{u}) = \text{const} \cdot \exp(-\tfrac{1}{2}m\beta_w u^2) \tag{1.11}$$

corresponding to particles desorbed thermally from a wall at an inverse temperature β_w different from the value β characterizing the medium in which the particles move. Temperature differences between the wall and the medium are to be expected when the "absorption" at the wall in the mathematical description corresponds physically to condensation in a layer adsorbed at the wall, or to some chemical reaction there (further comments on this issue are given in Section 6). When β and β_w differ by less than a factor of two, good results are obtained with a small number of functions $\chi_l(u_t)$; for larger discrepancies the convergence becomes markedly poorer for some physical quantities (see Section 4 for further details).

By combining the Milne and albedo problems we can treat the case of

partial absorption with *diffuse* thermal reflection of the nonabsorbed particles also for the case of differing bulk and wall temperatures. This is done in Section 5. We confirm an earlier finding[13] that the reflection mechanism, and not merely the reflection coefficient r, influences x_M, and hence the effective boundary condition to be used with the diffusion equation.

In the concluding section we first give a tentative explanation for the relatively rapid convergence of the moment method. We further discuss some possible generalizations, especially to more general forms of the collision operator $\mathscr{C}$ and to more realistic treatments of temperature differences between medium and wall. We include some first results for the simplest BGK operator of type (1.2). Finally, we briefly comment on the modifications needed to treat geometries of spherical, rather than planar, symmetry, a subject to be treated in a forthcoming paper.[14]

2. THE MOMENT METHOD AND ITS APPLICATION TO THE MILNE PROBLEM

The function $p_M(u_x, x)$ defined in (1.5) obeys the equation

$$\left[-u_x\frac{\partial}{\partial x}+\gamma\frac{\partial}{\partial u_x}\left(u_x+\frac{1}{m\beta}\frac{\partial}{\partial u_x}\right)\right]p_M(u_x, x)$$

$$\equiv[\mathscr{S}+\gamma\mathscr{C}]\,p_M(u_x, x)=0 \tag{2.1}$$

In the remainder of this paper we shall use units with $\gamma=m\beta=1$; this implies that lengths are measured in units of the velocity persistence length[15] $l=\gamma^{-1}(m\beta)^{-1/2}$, the analog of the mean free path for Brownian particles. Further, we shall denote u_x by u in the present and in the following section, where other components of $\mathbf{u}$ play no role. Equation (2.1) has two Chapman–Enskog-type solutions, the equilibrium solution

$$\Psi_0(u, x)=\phi_0(u)=\frac{1}{(2\pi)^{1/2}}\exp(-\tfrac{1}{2}u^2) \tag{2.2}$$

and a solution carrying a current -1,

$$\Psi_c(u, x)=(x-u)\,\phi_0(u) \tag{2.3}$$

There are additional solutions of the form

$$\Psi_{\pm n}(u, x)=[\exp(\mp x\lambda_n)]\,\psi_{\pm n}(u) \qquad \text{with} \quad \lambda_n=\sqrt{n} \tag{2.4}$$

and $\psi_{\pm n}(u)$ a set of functions first determined by Pagani,[16] also given in ref. 12. The function $p_M(u, x)$ must have the form

$$p_M(u, x) = \Psi_c(u, x) + \sum_{n=0}^{\infty} d_n^M \Psi_{+n}(u, x) \tag{2.5}$$

It was shown by Beals and Protopopescu[17] that there is a unique set of coefficients d_n^M such that $p_M(u, x)$ obeys the boundary condition

$$p_M(u, 0) = 0 \qquad \text{for} \quad u > 0 \tag{2.6}$$

The expansion (2.5) is not very suitable for numerical purposes, however; the approximants d_n^{MN} that minimize

$$\Delta_M = \int_0^{\infty} du\, u e^{u^2/2} \left[\Psi_c(u, 0) + \sum_{n=0}^{N} d_n^{MN} \Psi_{+n}(u, 0) \right]^2 \tag{2.7}$$

converge very slowly toward the exact d_n^M.[12,18]

It turns out to be advantageous to use *approximate* $\psi_{+n}(u)$ instead. These are obtained by first expanding $p_M(u, x)$ in the eigenfunctions $\phi_m(u)$ of $\mathscr{C}$ with eigenvalues $-m$,[15]

$$\phi_m(u) = \frac{1}{m!\,(2\pi)^{1/2}\, 2^{m/2}} e^{-u^2/2} H_m\left(\frac{u}{\sqrt{2}}\right) \tag{2.8}$$

where $H_m(\xi)$ is the mth Hermite polynomial. The streaming operator $\mathscr{S}$ can be written as[15]

$$\mathscr{S} = -[a_+ + a_-] \frac{\partial}{\partial x} \tag{2.9}$$

where the raising and lowering operators a_+ and a_- obey the relations

$$a_+ \phi_m = (m+1)\, \phi_{m+1}; \qquad a_- \phi_m = [1 - \delta_{m0}]\, \phi_{m-1} \tag{2.10}$$

By taking scalar products with the left eigenfunctions of $\mathscr{C}$ biorthonormal to the $\phi_n(u)$,

$$\tilde{\phi}_m(u) = \frac{1}{2^{m/2}} H_m\left(\frac{u}{\sqrt{2}}\right) \tag{2.11}$$

we can expand any function of u, and in particular the $\psi_n(u)$ (we henceforth omit the + sign in the index), in terms of the $\phi_m(u)$:

$$\psi_n(u) = \sum_{m=0}^{\infty} c_{nm} \phi_m(u) \tag{2.12}$$

In this representation the defining eigenvalue equation

$$[\mathscr{C} + \lambda(a_+ + a_-)]\,\psi_n(u) = 0 \tag{2.13}$$

becomes the set of recursion relations

$$m\lambda_n c_{n,m-1} - mc_{nm} + \lambda_n c_{n,m+1} = 0 \tag{2.14}$$

which can be written in matrix form as

$$\mathbb{K}(\lambda_n) \cdot \mathsf{c}_n = 0 \tag{2.15}$$

Since both $\mathscr{C}$ and $(a_+ + a_-)$ are Hermitian with respect to the scalar product

$$\langle \phi, \psi \rangle = (2\pi)^{1/2} \int du\, \phi(u)\, \psi(u)\, e^{u^2/2} \tag{2.16}$$

which translates into

$$\langle \phi, \psi \rangle = \sum_{m=0}^{\infty} \frac{1}{m!} c_{\phi m} c_{\psi m} \tag{2.17}$$

the eigenvalues λ_n of (2.15) must be real; from the invariance of (2.14) under the transformation

$$\lambda \to -\lambda; \qquad c_m \to (-1)^m c_m \tag{2.18}$$

one sees that they occur in pairs of opposite sign.

The approximate c_n^N used in our calculations are obtained by truncating the infinite matrix $\mathbb{K}(\lambda)$ at order $2N-1$. For $N=2$ we so obtain

$$\mathbb{K}^2(\lambda) \cdot \mathsf{c}^2 \equiv \begin{pmatrix} 0 & \lambda & 0 & 0 \\ \lambda & -1 & \lambda & 0 \\ 0 & 2\lambda & -2 & \lambda \\ 0 & 0 & 3\lambda & -3 \end{pmatrix} \begin{pmatrix} c_0^2 \\ c_1^2 \\ c_2^2 \\ c_3^2 \end{pmatrix} = 0 \tag{2.19}$$

Since the Hermiticity properties of $\mathbb{K}$ are preserved by the truncation, as is the invariance under (2.18), the eigenvalues of (2.19) are again real; they occur in pairs, but for the eigenvalue $\lambda_0 = 0$, which belongs to c_0^N with $c_{0m}^N = \delta_{m0}$, the representation of $\Psi_0(u, 0)$ defined in (2.2). We always find $N-1$ distinct positive eigenvalues, which we label λ_n^N $(n = 1, \ldots, N-1)$ in ascending order. The λ_n^N always exceed $\sqrt{n}$, but approach it from above as $N \to \infty$. The associated generalized eigenvectors c_n^N all have a nonvanishing c_{n0}^N, which is made equal to unity by the normalization of c_n^N,

and a vanishing c^N_{n1}. From (2.11) one sees that this implies that the approximants

$$\Psi^N_n(u, x) = \exp[-\lambda^N_n x] \sum_{m=0}^{2N-1} c^N_{nm} \phi_m(u) \tag{2.20}$$

all have unit density at the wall and zero current.

We now choose as the approximant of order N to the Milne solution $p_M(u, x)$ the expression

$$p^N_M(u, x) = \Psi_c(u, x) + \sum_{n=0}^{N-1} \alpha^{NM}_n \Psi^N_n(u, x) \tag{2.21}$$

where the α^N_n are chosen to obey the Marshak condition[9]

$$\int_0^\infty du\, p^N_M(u, 0)\, u^{2k+1} = 0 \qquad \text{for} \quad 0 \leqslant k \leqslant N-1 \tag{2.22}$$

For $N \to \infty$ this becomes equivalent to (2.6): since the powers u^k are complete on $(-\infty, +\infty)$, the odd powers alone (or the even powers alone) are complete on $(0, \infty)$. Using (2.21), (2.20), and (2.3), we can write the conditions (2.22) as

$$\sum_{n=0}^{N-1} \alpha^{NM}_n \sum_{m=0}^{2N-1} c^N_{nm} M^k_m = M^k_1, \qquad 0 \leqslant k \leqslant N-1 \tag{2.23}$$

with

$$M^k_m = \int_0^\infty du\, u^{2k+1} \phi_m(u) \tag{2.24}$$

These N conditions allow one to determine the N coefficients α^N_n.

The approximants $p^{10}_M(u, 0)$, $p^{20}_M(u, 0)$, and $p^{30}_M(u, 0)$ are shown in Fig. 1. These functions come closer to fulfilling (2.6) than the approximants using 35, 70, and 140 exact $\psi_n(u)$, given in Fig. 2 of ref. 12. For not too small negative u, good convergence is obtained. The same holds for the approximate density profile

$$n^N_M(x) = \int du\, p^N_M(u, x) = x + \alpha^{NM}_0 + \sum_{n=1}^{N-1} \alpha^{NM}_n \exp[-\lambda^N_n x] \tag{2.25}$$

[One sees that α^{NM}_0 goes to the Milne length x_M defined in (1.8).] For large enough N the α^{NM}_0 and $n^N_M(x)$ depend smoothly and monotonically

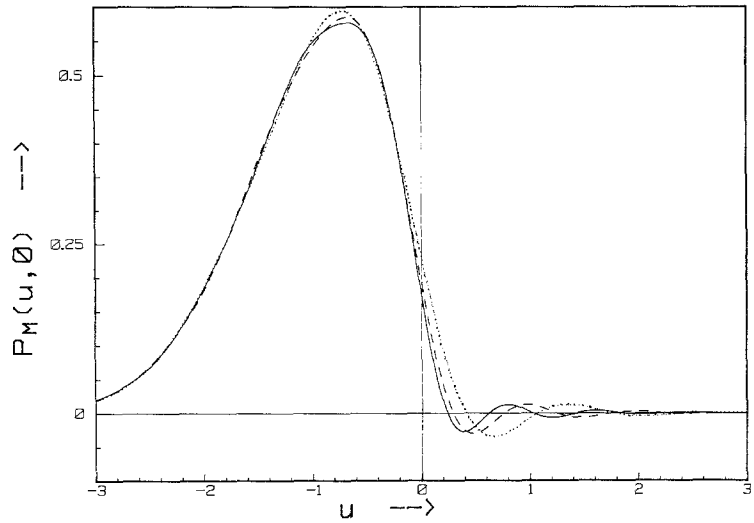

Fig. 1. The distribution $P_M(u, 0)$ of the velocity normal to the wall at a fully absorbing wall, as approximated using 10 (dotted line), 20 (dashed line), and 30 (solid line) moments. The exact solution vanishes for $u > 0$.

on N, and we can use the empirical extrapolation (1.7). For x_M we find an exponent $\delta \approx 1.5$ and an estimate

$$x_M^\infty = 1.46035 \pm 0.00001 \tag{2.26}$$

where the error is determined by comparing fits of type (1.7) for different groups of five successive N values.[2] Our result (2.26) agrees with the exact result[4] $x_M = -\zeta(1/2)$ to the precision given. In a double-precision calculation (16 significant digits) the quality of the approximants decreases beyond $N \simeq 25$ due to the effect of roundoff errors, which are amplified by the large differences in magnitude of the coefficients in (2.23). The same procedure works for $n_M(x)$, though the convergence exponent is smaller ($\delta \simeq 0.75$ for $x = 0$), and the number of significa... ...igures obtained is less. The results for the boundary layer part of the profile, $|n_M(x) - x - x_M|$, are given in Table I, together with the exact results of Marshall and Watson,[4] with which they agree to within the numerical error. In particular, the nonanalytic behavior of $n_M(x)$ near $x = 0$,

$$n_M(x) \simeq n_M(0) + (2/\pi)^{1/4} \sqrt{x} + \mathcal{O}(x) \tag{2.27}$$

[2] If there is a definite trend in these extrapolations, a second fit of type (1.7) is used to obtain a better estimate.

Table I. The Boundary Layer Part of the Density Profile $-n_b(x) = |n_M(x) - x - x_M|$ at a Fully Absorbing Wall for Several Values of x[a]

x	0	2^{-8}	2^{-6}	2^{-4}	2^{-2}	1
Present method	0.524	0.47	0.41*	0.334	0.201	0.06011
Exact solution[4]	0.52424	0.47056	0.41516	0.33386	0.20120	0.06011

[a] The estimated error is one unit in the underlined digit; an asterisk signifies that no reliable error estimate can be given.

is reproduced very well. This is somewhat surprising, since the small-x behavior of the approximants $n_M^N(x)$ is dominated by the contributions of the $\Psi_n^N(u, x)$ in (2.21) with n close to N. These approximate generalized eigenfunctions of (2.15) are heavily influenced by the truncation, and bear no resemblance to any of the actual $\Psi_n(u, x)$. Still, they are apparently successful in helping to mimic the true behavior of $n_M(x)$.

3. PARTIALLY REFLECTING WALLS

In this section we generalize some of the results of the preceding section to the case of a partially reflecting wall. We shall confine ourselves here to the case of *specular* reflection, with a reflection coefficient r that does not depend on the velocity $\mathbf{u}$ at impact. This implies that the solution still has the general form (1.5). (We shall consider more general types of reflection in Section 5.) The required solution $p_{Mr}(u, x)$ must satisfy the boundary condition[12]

$$p_{Mr}(u, 0) = r p_{Mr}(-u, 0) \qquad \text{for} \quad u > 0 \tag{3.1}$$

This problem provides a sensitive test for the moment procedure, since the function $p_{Mr}(u, x)$ is known to be even more strongly nonanalytic at $u = x = 0$ than $p_M(u, x)$. For small $|u|$ one has, e.g.,[19]

$$p_{Mr}(u, 0) \approx \text{const} \cdot |u|^{\alpha(r)} [\Theta(-u) + r\Theta(u)] \tag{3.2}$$

with

$$\alpha(r) = \frac{1}{2} - \frac{3}{\pi} \arcsin\left(\frac{r}{2}\right) \tag{3.3}$$

whereas the density profile $n_{Mr}(x)$ has the form

$$n_{Mr}(x) = n_{Mr}(0) + \text{const} \cdot x^{[1+\alpha(r)]/3} + \mathcal{O}(x) \tag{3.4}$$

We determined approximants $p_{Mr}^N(u, x)$ by the method of Section 2, with the boundary condition (3.1) replaced by

$$\int_0^\infty du\, u^{2k+1} p_{Mr}(u, 0) = r \int_{-\infty}^0 du\, |u|^{2k+1} p_{Mr}(u, 0); \qquad 0 \leqslant k \leqslant N-1 \quad (3.5)$$

The results for $N = 25$ and some values of r are shown in Fig. 2. Not surprisingly, one sees only a vague indication of the singular behavior (3.2) in these analytic approximants. For not too small $|u|$ we find good convergence, however. In Fig. 3 we show the approximants to $n_{Mr}(x)$, multiplied with x_M/x_{Mr} for ease of comparison. The values of x_{Mr} used are obtained by extrapolation of the x_{Mr}^N using the fit (1.7). Also indicated in the figure are the extrapolated wall densities $n_{Mr}^\infty(0)$. The steepening of the profile with increasing r, read off from (3.4), is also clearly indicated by the approximants shown in the figure.

The extrapolated values for x_{Mr} and the scaled density at the wall

$$d_{Mr} \equiv n_{Mr}(0)/x_{Mr} \quad (3.6)$$

are given in Table II, together with the respective convergence exponents δ. The latter decrease with increasing r. This is not unexpected, since the convergence exponents for the variational method of ref. 12, which are

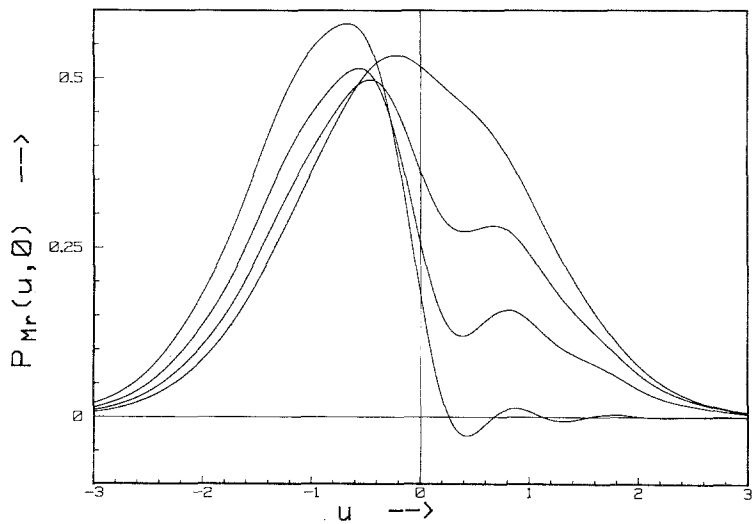

Fig. 2. The velocity distributions $p_{Mr}(u, 0)$ at a partially absorbing wall with specular reflection, for values $r = 0$, 0.3, 0.6, and 0.9 of the reflection coefficient, as approximated with 25 moments. The values of r increase in the same direction as the $p_{Mr}(u, 0)$ for $u > 0$.

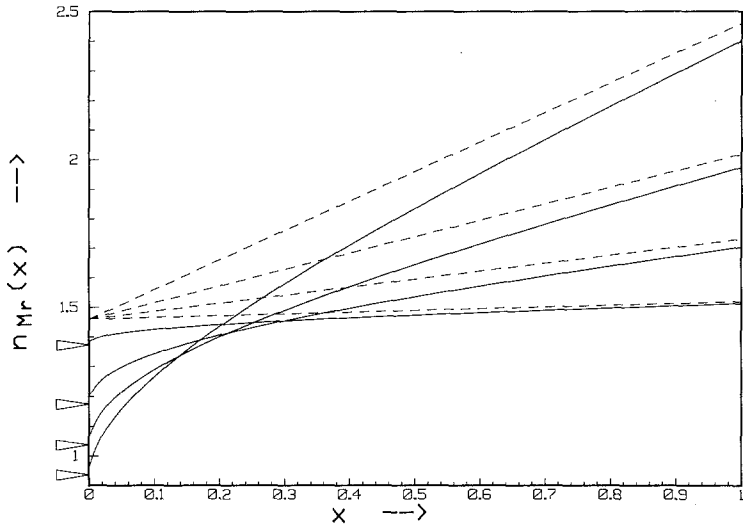

Fig. 3. The density profile $n_{Mr}(x)$ near a partially absorbing wall at $x=0$, with specular reflection and reflection coefficients $r=0$, 0.3, 0.6, and 0.9, approximated with 25 moments. The arrows indicate the extrapolated densities at the wall; the dashed curves are the asymptotes $n_{as}(x)=x_M(x+x_{Mr})/x_{Mr}$. The solutions are normalized such that the asymptotes all intersect at $x=x_{M0}$; the values of r increase with decreasing steepness of the profiles.

smaller by roughly a factor of three, can be shown to follow a similar trend.[20] We also include the lowest approximant x^1_{Mr}, equal to an expression proposed by Bethe *et al.*[21] for a similar problem, and given by

$$x^1_{Mr}=\frac{1+r}{1-r}\left(\frac{\pi}{2}\right)^{1/2} \tag{3.7}$$

It is obtained from the Chapman–Enskog-type trial function

$$p^1_{Mr}(u,x)=\Psi_c(u,x)+x^1_{Mr}\Psi_0(u,x) \tag{3.8}$$

Table II. The Milne Length x_{Mr} and the Relative Density at the Wall $d_{Mr}=n_{Mr}(0)/x_{Mr}$, with Their Convergence Exponents, for Partially Absorbing Walls with Specular Reflection, As a Function of the Reflection Coefficient r[a]

r	x_{Mr}	δ_x	x^1_{Mr}	$d_r(0)$	δ_d
0	1.46035	1.5	1.2533	0.641	0.75
0.3	2.6165	1.4	2.3276	0.711	0.71
0.6	5.3991	1.25	5.0133	0.805	0.63
0.9	24.317	1.1	23.813	0.9399	0.55

[a] The simple estimate x^1_{Mr} is given for comparison. Errors are indicated as in Table I.

The difference $(x_{Mr} - x^1_{Mr})$ gives an indication of the importance of the kinetic boundary layer for the value of x_{Mr}. This importance is seen to decrease with increasing r (which means decreasing frustration of the approach toward local thermal equilibrium by the boundary condition).

We conclude this section with a remark on the significance of the parameter x_{Mr}. The asymptotic density profile

$$n^{\text{as}}_{Mr}(x) = x + x_{Mr} \tag{3.9}$$

clearly obeys the boundary condition

$$\left.\frac{\partial n^{\text{as}}_{Mr}(x)}{\partial x}\right|_{x=0} = \frac{1}{x_{Mr}} n^{\text{as}}_{Mr}(0) \tag{3.10}$$

when extrapolated toward $x = 0$. Moreover, it clearly satisfies the stationary diffusion equation

$$\frac{\partial^2}{\partial x^2} n^{\text{as}}(x) = 0 \tag{3.11}$$

as required for a density belonging to a Chapman–Enskog-type solution of the Kramers equation.[15] This suggests using the boundary condition (3.10) with the time-dependent diffusion equation

$$\frac{\partial}{\partial t} n^{\text{as}}(x, t) = \frac{\partial^2}{\partial x^2} n^{\text{as}}(x, t) \tag{3.12}$$

to determine the density associated with a time-dependent solution of the Klein–Kramers equation in the hydrodynamic stage (for values of x not too close to the wall). This recipe, which can be justified more fully,[20] is an example of the extraction of a boundary condition for a hydrodynamic equation from a boundary condition on the kinetic level.

4. THE ALBEDO PROBLEM

In this section we consider the case that the wall at $x = 0$ acts as a source of Brownian particles: particles with velocity $\mathbf{u}$ are injected into the medium at a constant rate, independent of y and z, which we denote by $u_x\, g(\mathbf{u})$. The particles are removed from the system when they return to the wall. A diffusing particle is certain to reach the plane of origin again eventually[4] (this is a variant of the well-known "gambler's ruin theorem"). Hence, in the stationary state there are as many particles returning to the wall as there are injected: no net current flows unless there are sources at

infinity. From this one sees that there is a second possible physical interpretation: no particles are created or absorbed at the wall, but any particle hitting the wall is reflected back into the medium *in a completely diffuse way*, so that the probability distribution of reentrance velocities is completely independent of the impact velocity. To obtain a nontrivial stationary state, this distribution of reentrance velocities must of course differ from the equilibrium distribution $\phi_0(\mathbf{u}) = \phi_0(u_x)\,\phi_0(u_y)\,\phi_0(u_z)$. Whatever the interpretation, the stationary distribution, called $P_g(\mathbf{u}, x)$ must obey the Klein–Kramers equation with the boundary condition[22]

$$P_g(\mathbf{u}, 0) = g(\mathbf{u}) \qquad \text{for} \quad u_x > 0 \tag{4.1}$$

The solution of this problem is greatly simplified because the collision operator $\mathscr{C}$ can be written as

$$\mathscr{C} = \mathscr{C}_x + \mathscr{C}_y + \mathscr{C}_z; \qquad \mathscr{C}_i = \frac{\partial}{\partial u_i}\left[u_i + \frac{\partial}{\partial u_i}\right] \tag{4.2}$$

Since $P_g(\mathbf{u}, x)$ does not depend on y or z, $\mathscr{S}$ contains only u_x, and it is advantageous to expand $g(\mathbf{u})$ and $P_g(\mathbf{u}, x)$ in the common eigenfunctions of $\mathscr{C}_y$ and $\mathscr{C}_z$. We shall not work out the general case, but assume that $g(\mathbf{u})$, and hence $P(\mathbf{u}, x)$, depends on u_y and u_z only via

$$u_t = (u_y^2 + u_z^2)^{1/2} \tag{4.3}$$

When acting on such functions, $\mathscr{C}$ can be replaced by

$$\mathscr{C} = \mathscr{C}_x + \mathscr{C}_t \tag{4.4}$$

with

$$\mathscr{C}_t = \frac{1}{u_t}\frac{\partial}{\partial u_t} u_t \left[u_t + \frac{\partial}{\partial u_t}\right] \tag{4.5}$$

[for general $g(\mathbf{u})$, (4.4) has to be supplemented by a term $\mathscr{C}_\phi$ acting on the orientation of the two-dimensional vector (u_y, u_z)].

One readily checks that the function $\chi_l(u_t)$ defined as

$$\chi_l(u_t) = \frac{1}{2\pi l!} \exp(-\tfrac{1}{2}u_t^2)\, L_l(\tfrac{1}{2}u_t^2) \tag{4.6}$$

with $L_l(\xi)$ the lth Laguerre polynomial, are eigenfunctions of $\mathscr{C}_t$ with eigenvalues $-2l$:

$$\mathscr{C}_t \chi_l(u_t) = -2l\chi_l(u_t) \tag{4.7}$$

From the properties of the Laguerre polynomials and the Hermiticity of $\mathscr{C}_t$ with respect to the scalar product

$$\langle f, g \rangle_t = 2\pi \int du_t\, u_t \exp(\tfrac{1}{2}u_t^2)\, f(u_t)\, g(u_t) \tag{4.8}$$

one sees that the eigenfunctions biorthonormal to the χ_l are

$$\tilde{\chi}_l(u_t) = 2\pi \exp(\tfrac{1}{2}u_t^2)\, \chi_l(u_t) \tag{4.9}$$

By taking (4.8)-type scalar products with the $\tilde{\chi}_l$, one decomposes both $P_g(\mathbf{u}, x)$ and $g(\mathbf{u})$:

$$P_g(u_x, u_t, x) = \sum_l p_{gl}(u_x, x)\, \chi_l(u_t) \tag{4.10}$$

$$g(u_x, u_t) = \sum_l g_l(u_x)\, \chi_l(u_t) \tag{4.11}$$

The $p_{gl}(u_x, x)$ clearly must obey the modified Klein–Kramers equation

$$\left[-u_x \frac{\partial}{\partial x} + \mathscr{C}_x - 2l \right] p_{gl}(u_x, x) = 0 \tag{4.12}$$

and the boundary condition

$$p_{gl}(u_x, 0) = g_l(u_x) \qquad \text{for} \quad u_x > 0 \tag{4.13}$$

The solution of this boundary layer problem is again found by writing $p_{gl}(u_x, x)$ as [cf. (2.21)]

$$p_{gl}(u_x, x) = \sum_{n=0}^{\infty} d_n^{gl} \Psi_{nl}(u_x, x) \tag{4.14}$$

with

$$\Psi_{nl}(u_x, x) = \exp(-\lambda_{nl} x)\, \psi_{nl}(u_x) \tag{4.15}$$

and λ_{nl} and $\psi_{nl}(u)$ the positive eigenvalues and corresponding eigenfunctions of the generalized eigenvalue problem

$$[\mathscr{C}_x - 2l + \lambda_{nl}(a_{+x} + a_{-x})]\, \psi_{nl}(u_x) = 0 \tag{4.16}$$

The exact $\psi_{nl}(u_x)$ and λ_{nl} can be found by a straightforward adaptation of Pagani's method[16] (see also ref. 23). The results are

$$\psi_{nl}(u_x) = \text{const} \cdot H_n\left[\frac{1}{\sqrt{2}} \{u_x - [2(n+2l)]^{1/2}\} \right] \times \exp\left\{ -\frac{1}{2} [u_x - (n+2l)^{1/2}]^2 \right\} \tag{4.17}$$

$$\lambda_{nl} = (n+2l)^{1/2} \tag{4.18}$$

As in the Milne case, we construct approximants to $p_{gl}(u_x, x)$ of the form

$$p_{gl}^N(u_x, x) = \sum_{n=0}^{N-1} \alpha_n^{Ngl} \Psi_{nl}^N(u_x, x) \tag{4.19}$$

with

$$\Psi_{nl}^N(u_x, x) = \exp(-\lambda_{nl}^N x) \sum_{m=0}^{2N-1} c_{nlm}^N \phi_m(u_x) \tag{4.20}$$

The c_{nlm}^N are determined as in Section 2, with $\mathbb{K}(\lambda)$ in (2.15) replaced by $\mathbb{K}(\lambda) - 2l\mathbb{I}$, and the α_n^{Ngl} follow from the Marshak-type conditions

$$\int_0^\infty du_x\, u_x^{2k+1} \Psi_{nl}^N(u_x, 0) = \int_0^\infty du_x\, u_x^{2k+1} g_l(u_x); \qquad 0 \leqslant k \leqslant N-1 \tag{4.21}$$

As before, c_{nl0}^N can be shown to be nonzero, and we normalize $\mathbf{c}_{nl}^N$ such that c_{nl0}^N equals unity.

We carried out some calculations for the special case

$$g(\mathbf{u}) = \frac{\beta_w^2}{2\pi} e^{-\beta_w u^2/2} \Theta(u_x) \tag{4.22}$$

where the normalization is chosen such that a unit current j_+ is injected into the medium. The corresponding $g_l(u_x)$ are

$$g_l(u_x) = \beta_w e^{-\beta_w u^2/2} \left(1 - \frac{1}{\beta_w}\right)^l \tag{4.23}$$

Good convergence is obtained for the individual expansion coefficients α_n^{Ngl} defined in (4.19), as well as for the density profile

$$n_g(x) = \sum_{n=0}^{\infty} d_n^{g0} e^{-\lambda_{n0} x} \tag{4.24}$$

In Table III we give $n(0)$ and $n(\infty) = d_0^{g0}$ for $\beta_w = 0.5$ and $\beta_w = 2$. [For $\beta_w = 1$ one obtains the flat profile $n(x) = (2\pi)^{1/2} \simeq 2.5066$.] The increase of

Table III. The Density at the Wall, $n(0)$, and at Infinity, $n(\infty)$, with Their Convergence Exponents, for the Albedo Problem with a Thermal Source of Unit Strength, at Two Relative Inverse Temperatures β_w [a]

β_w	$n(0)$	δ_0	$n(\infty)$	δ_∞
0.5	2.009	0.66	3.0940	1.66
2.0	3.230	0.77	2.0565	1.66

[a] For $\beta_w = 1$ both values are $(2\pi)^{1/2} \simeq 2.50663$. Errors are indicated as in Table I.

$n(\infty)$ with increasing $T_w = \beta_w^{-1}$ is reasonable: the higher the injection velocity, the longer the distance the particle travels before it has lost the memory of its initial velocity, and the lower its probability for a rapid return to the wall. The general form of the density profile can be understood from the temperature profiles and the relation[12]

$$n_g(x)\, T_{xg}(x) \equiv \int d\mathbf{u}\, P_g(\mathbf{u}, x)\, u_x^2 = n_g(\infty) \tag{4.25}$$

which is proved in the Appendix. The profiles for $T_{xg}(x)$ and the analogous transverse quantity

$$T_{tg}(x) = \frac{1}{n_g(x)} \frac{1}{2} \int d\mathbf{u}\, P_g(\mathbf{u}, x)\, u_t^2 \tag{4.26}$$

are shown in Fig. 4. [The density profiles can be determined from those of $T_{xg}(x)$ using (4.25).] As expected, both $T_{xg}(x)$ and $T_{tg}(x)$ approach unity (the medium temperature) for $x \to \infty$. The approach is faster for $T_{tg}(x)$; this is clear from the explicit expressions for $T_{xg}(x)$ and $T_{tg}(x)$ in the Appendix, but also intuitively: u_x and u_t are uncorrelated, both in their initial distribution and in their decay, and only a high starting value of u_x

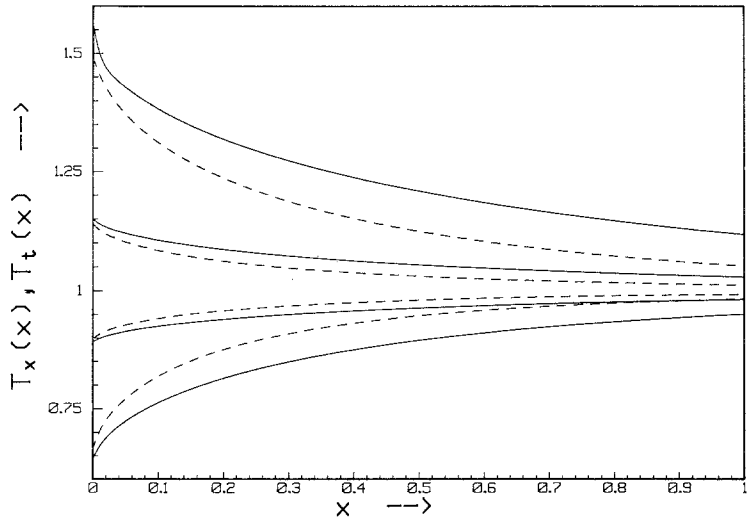

Fig. 4. Profiles for the normal temperature $T_x(x)$ (solid lines) and the transverse temperature $T_t(x)$ (dashed lines) near a diffusely reflecting wall at an inverse temperature β_w different from the value β in the medium. Approximants are calculated with 30 moments, and for $\beta_w/\beta = 0.5$, 0.8, 1.2, and 2. The higher curves correspond to the lower values of β_w/β. Note that neither $T_i(x)$ approaches β_w^{-1} at the wall.

helps the particle to penetrate deeply before it loses memory of its initial velocity. Note also that the $T_{ig}(x)$ do not approach β_w^{-1} for $x \to 0$. This temperature jump reflects the fact that only particles leaving the wall have a temperature β_w^{-1}; the returning particles have thermalized to some extent.

The full distribution functions $P_g(\mathbf{u}, x)$ contain contributions from all $\chi_l(u_t)$, hence one has to consider their convergence properties both with respect to l and with respect to N. These properties were studied in some detail,[24] but we give only the main features. For β_w not too different from unity, good convergence is obtained with a small number of χ_l (6 or at most 11). As before, the singular structure at $u_x = x = 0$ is not reproduced very well, but the error decreases with increasing u_t. As an illustration we show in Fig. 5 the approximant to $P(u_x, u_t, 0)$ for $\beta_w = 1.2$ with $l_{\max} = 5$ and $N = 30$, together with the "target function" $g(u_x, u_t)\,\Theta(u_x)$. For $\beta_w \lesssim 0.5$ or $\beta_w \gtrsim 2$ the convergence for the distribution function becomes markedly worse. In particular, the approximants for fixed $l_{\max}$ show oscillatory convergence with N; for $\beta_w = 2$ and $u_t = 0$, no convergence is seen before roundoff errors make the results unreliable. For $\beta_w \leqslant 0.5$ no convergence with $l_{\max}$ is seen (for part of the range), as could have been expected from (4.23). Note, however, that even poor convergence of the distribution function does not preclude an accurate determination of some of its moments, such as the density or the temperature.

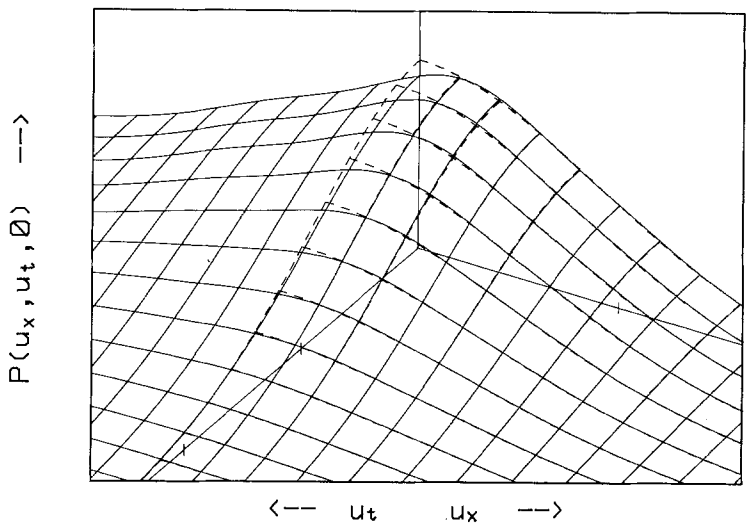

Fig. 5. The distribution $P(u_x, u_t, 0)$ at a wall with $\beta_w = 1.2$; the boundary condition to be fulfilled for $u_x > 0$ is drawn with dashed lines where it deviates from the approximant obtained with 30 moments in u_x and 6 in u_t. Note the slower decay with $|u_x|$ (higher temperature) of the returning particles ($u_x < 0$) compared with the injected ones ($u_x > 0$).

5. DIFFUSE PARTIAL REFLECTION

The case considered in Section 3 is only a special case of a partially reflecting wall. The most general model is obtained by specifying a probability $\sigma(\mathbf{u}|\mathbf{u}')$ that a particle hitting the wall with velocity $\mathbf{u}'$ is reinjected with velocity $\mathbf{u}$. The corresponding boundary condition for the Klein–Kramers equation is[13,22]

$$u_x P(\mathbf{u}, 0) = \int_{u'_x < 0} d\mathbf{u}'\, \sigma(\mathbf{u}|\mathbf{u}')\, |u'_x|\, P(\mathbf{u}', 0); \qquad u_x > 0 \tag{5.1}$$

The associated reflection coefficient $r(\mathbf{u}')$ can be defined as

$$r(\mathbf{u}') = \int d\mathbf{u}\, \sigma(\mathbf{u}|\mathbf{u}') \tag{5.2}$$

and the absorption probability equals $a(\mathbf{u}') = 1 - r(\mathbf{u}')$; we shall always assume that $r(\mathbf{u}')$ is less than or equal to unity, and exclude the case $r(\mathbf{u}') \equiv 1$, already treated in Section 4.

We postpone the discussion of the general case till later in this section and first consider the case of a separable $\sigma(\mathbf{u}|\mathbf{u}')$:

$$\sigma(\mathbf{u}|\mathbf{u}') = u_x\, g(\mathbf{u})\, r(\mathbf{u}'); \qquad \int d\mathbf{u}\, u_x\, g(\mathbf{u}) = 1 \tag{5.3}$$

Physically this means that the velocity distribution of the reinjected particles is independent of $\mathbf{u}'$. Hence we shall call (5.3) the *diffuse reflection* case. For this case the solution carrying a unit current in the negative x direction has the form

$$P_\sigma(\mathbf{u}, x) = P_M(\mathbf{u}, x) + A_r P_g(\mathbf{u}, x) \tag{5.4}$$

where P_M and P_g are the Milne and albedo solutions constructed in Sections 2 and 4, respectively, and A_r is a constant that can be determined by substitution of (5.3), (5.4), and (1.4) into (5.1), and integration over $\mathbf{u}$:

$$A_r = \int_{u'_x < 0} d\mathbf{u}'\, |u'_x|\, r(\mathbf{u}')[P_M(\mathbf{u}', 0) + A_r P_g(\mathbf{u}', 0)] \tag{5.5}$$

For an $r(\mathbf{u}')$ independent of $\mathbf{u}'$ this takes the simple form

$$A_r = r(1 + A_r) \qquad \text{or} \qquad A_r = r/(1 - r) \tag{5.6}$$

From (5.4) one immediately derives expressions for $n(x)$, and in particular for the Milne length:

$$x_{Mrg} = x_M + A_r d_0^{g0} \tag{5.7}$$

Table IV. The Milne Length x_{Mrg} for Partially Absorbing Walls with Diffuse Reflection As a Function of Reflection Coefficient r and Inverse Wall Temperature β_w [a]

	x_{Mrg}			
r	$\beta_w = 0.5$	$\beta_w = 1$	$\beta_w = 2$	x_{Mr}
0.3	2.7864	2.53462	2.3417	2.6165
0.6	6.1014	5.22029	4.5451	5.3991
0.9	29.306	24.0200	19.969	24.317

[a] The values for specular reflection x_{Mr} are given for comparison. Errors are indicated as in Table I.

The values for x_{Mrg} for some values of r and some $g(\mathbf{u})$ discussed in Section 4 are given in Table IV, together with the values x_{Mr} from Section 3. One sees that the effective boundary condition in (3.10) depends not only on the reflection coefficient r, but also on further details of the reflection mechanism.

The profiles for $T_{t\sigma}(x)$ follow immediately from the $n(x)$ and $n(x)\, T_t(x)$ derived from (5.4) [note that $T_t(x) = 1$ for $P_M(\mathbf{u}, x)$]

$$T_{t\sigma}(x) = \frac{n_M(x) + A_r n_g(x)\, T_{tg}(x)}{n_M(x) + A_r n_g(x)} \tag{5.8}$$

The calculation of $T_{x\sigma}(x)$ is somewhat more involved, however, since $\langle u_x \rangle$ no longer vanishes, and one must use the definition

$$T_x = \langle u_x^2 \rangle - \langle u_x \rangle^2 \tag{5.9}$$

The quantity $\langle u_x \rangle$ vanishes for $P_g(\mathbf{u})$, but for $P_M(\mathbf{u})$ one has

$$j_{xM} = \int d\mathbf{u}\, u_x P_M(\mathbf{u}, x) = n_M(x) \langle u_x \rangle_M (x) = -1 \tag{5.10}$$

The resulting expression for $T_{x\sigma}(x)$ is written out in the Appendix, where we also give expressions for $n_\sigma(x)$, $T_{t\sigma}(x)$, and $T_{x\sigma}(x)$ in terms of the α_n^{NM} and the α_n^{Ngl}. In Fig. 6 we give an example of the resulting profiles $T_{x\sigma}(x)$ and $T_{t\sigma}(x)$. In $T_{x\sigma}(x)$ the cooling influence of the constituent P_M in (5.4) counteracts the heating influence of the P_g contribution for a hot wall; for not too large r the former is dominant. Further examples of density and temperature profiles are given in ref. 24.

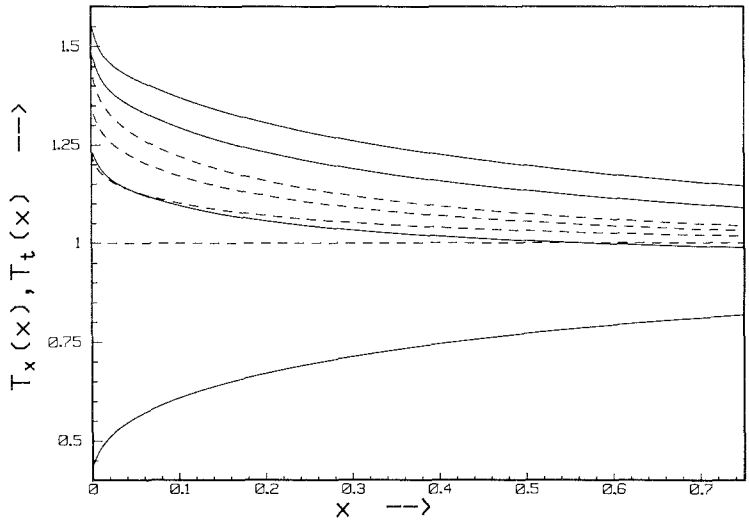

Fig. 6. The temperature profiles $T_x(x)$ (solid lines) and $T_t(x)$ (dashed lines) near a partially absorbing wall with diffuse reflection at a temperature twice that of the medium, for reflection coefficients $r=0$, 0.3, 0.6, and 0.9. The higher curves correspond to the higher reflection coefficients.

To conclude this section, we briefly consider the general case (5.1). When $\sigma(\mathbf{u}, \mathbf{u}')$ is invariant under a simultaneous rotation of $\mathbf{u}$ and $\mathbf{u}'$ around the u_x axis, the solution may be written as

$$P_\sigma(u_x, u_t, x) = \sum_{l=0}^{\infty} p_{\sigma l}(u_x, x)\, \chi_l(u_t) \tag{5.11}$$

The $p_{\sigma l}(u_x, x)$ with $l>0$ must vanish for $x \to \infty$, whereas

$$p_{\sigma 0}(u_x, x) \simeq \Psi_c(u_x, x) + x_{M\sigma}\phi_0(u_x) \qquad (x \gg 1) \tag{5.12}$$

with $x_{M\sigma}$ to be determined. At $x=0$ one has the boundary conditions

$$u_x p_{\sigma l}(u_x, 0) = \sum_{l'=0}^{\infty} \int_{-\infty}^{0} du'_x\, \sigma_{ll'}(u_x | u'_x)\, |u'_x|\, p_{\sigma l'}(u'_x, 0) \qquad (u_x > 0) \tag{5.13}$$

with

$$\sigma_{ll'}(u_x | u'_x) = \int d\mathbf{u}_t \int d\mathbf{u}'_t\, \tilde{\chi}_l(u_t)\, \chi_{l'}(u'_t)\, \sigma(\mathbf{u} | \mathbf{u}') \tag{5.14}$$

where $d\mathbf{u}_t$ stands for $du_y\, du_z$ and $d\mathbf{u}'_t$ for $du'_y\, du'_z$. The coupling between the various l makes for a quite complicated numerical problem. A tractable case of some practical importance arises for a mixture of diffuse and specular reflection

$$\sigma(\mathbf{u}\,|\,\mathbf{u}') = r_d u_x\, g(u_x, u_t) + r_s \delta(u_x + u'_x)\, \delta(\mathbf{u}_t - \mathbf{u}'_t) \tag{5.15}$$

In this case the solution is a linear combination of $P_{Mr_d}(\mathbf{u}, x)$ discussed in Section 3 and a multiple of the modified albedo solution $P_{gr_s}(\mathbf{u}, x)$ obeying

$$P_{gr_s}(u_x, u_t, 0) = g(\mathbf{u}) + r_s P_{gr_s}(-u_x, u_t, 0) \qquad (u_x > 0) \tag{5.16}$$

In the latter problem the equations for different l decouple again, and only the $l = 0$ component is needed to determine the coefficient $A_{gr_d r_s}$ of (5.16) in the full solution.

6. CONCLUDING REMARKS

In this section we shall first comment on the successes and shortcomings of our method and on its applicability to more general collision operators. In that context we present first results for the application to the BGK collision operator (1.2). Next we compare our results for the effective boundary condition in (3.10) with some recent proposals in the literature. We then sketch some ideas for a more realistic treatment of problems in which wall and medium are at different temperatures. Finally, we discuss the extension of our treatment to different geometries, especially to the problem of a (partially) absorbing sphere, treated more fully in a forthcoming paper.[14]

The advantage of replacing expansions of type (2.5) in terms of the exact boundary layer functions (used also in the exact solution[3,4]) by a sequence of expansions of type (2.25) in terms of approximate boundary layer eigenfunctions is the much faster convergence of the latter procedure. A tentative (and certainly far from rigorous) understanding of this phenomenon can be obtained by considering (4.17), which for $l = 0$ becomes the $\psi_n(u)$ used in (2.5). It has n zeros, all lying in the interval $(0, (8n)^{1/2})$. Thus, truncating (2.5) at order N roughly corresponds to cutting off a Fourier transform at $k_c^N \sim N^{1/2}$ [the dominant wavelength in $\psi_n^N(u)$ roughly equals the spacing of its zeros]. The highest approximate eigenvalue λ_{N-1}^N, on the other hand, turns out to be of order $N^{3/2}$ (compared to $N^{1/2}$ for the exact λ_{N-1}), and the zeros of the associated approximate eigenfunction have a correspondingly smaller spacing. Thus, the highest Fourier component taken into account, albeit in a very rough way, is of order $N^{3/2}$. Since all $P(u, 0)$ considered in this paper are non-

analytic at $u=0$, their Fourier transforms in general decrease like $k^{-\alpha}$ for large k with α varying from case to case; thus, the cutoff errors for moments of $P(u, 0)$ can be expected to vary also like some inverse power of k_c, say like $k_c^{-\gamma}$. Thus, it appears not unreasonable that the convergence exponent δ in fits of type $\alpha^N = \alpha^\infty + \alpha' N^{-\delta}$ should about triple after replacement of the exact by the approximate eigenfunctions, which is roughly what we find.

The main disadvantage of our method is its reliance on fits of type (1.7). One knows[18] that the errors made in the scheme of ref. 12 behave in this way asymptotically for large N, though logarithmic corrections are known to occur for some special albedo problems.[20] For our approximation scheme there is no such theorem, and the fit (1.7) is merely heuristic, though no errors were found to arise from it for quantities known exactly. However, occasionally we did not succeed, due to accumulating roundoff errors, to go high enough in N to reach the asymptotic region. The situation might be improved by using extended precision, or conceivably by optimization of some of our algorithms. Some features of the solution, however, in particular the singularity structure near $u=x=0$, are probably easier to determine by applying asymptotic analysis[18] or by evaluating the exact solution.

The main advantage of our method is its relative insensitivity, at least in principle, to the detailed structure of the collision operator $\mathscr{C}$. Of course, there is no guarantee that the same favorable convergence properties will be found for arbitrary $\mathscr{C}$. As a first test in this respect we treated an exactly solved case of BGK type, namely the BGK operator for a highly diluted impurity species in a carrier gas in thermal equilibrium:

$$\mathscr{C}P(\mathbf{u}, x) = -\gamma[P(\mathbf{u}, x) - \phi_0(\mathbf{u}) \int d\mathbf{u}'\, P(\mathbf{u}', x)] \tag{6.1}$$

where $\phi_0(\mathbf{u})$ stands for the three-dimensional Maxwell distribution at the temperature of the carrier gas. The Milne problem for this case (or rather a combination of Milne and albedo problem of the kind treated in Section 5) was shown to be reducible to the Kramers problem[2] by Ytrehus *et al.*[25] The exact value for the Milne length is thus equal to the slip coefficient (with the dimension of a length) for the Kramers problem, which in our units is

$$x_M^{\mathrm{BGK}} = 1.43705\ldots \qquad \text{(exact)}$$

The value we obtain is

$$x_M^{\mathrm{BGK}} = 1.4371 \pm 0.0001 \qquad \text{(moment method)}$$

The agreement is the more remarkable since the exact spectrum of relaxation lengths λ is continuous, apart from the discrete eigenvalue $\lambda = 0$, and extends from 0 to ∞; the associated generalized eigenfunctions are highly singular.[2] Thus, our approximate $\Psi_n^N(u, x)$ [cf. (2.20)] do not correspond to any identifiable feature of the exact solution. Our results for the density $n_M(x)$ at some values of x are given in Table V, together with the exact results of ref. 25. For higher values of x no error estimate can be given, since the range of N for which (1.7) applies is not large enough. The agreement between our method and the exact results is somewhat less impressive than in Table I. This may be due to the shortness of the asymptotic region in N. Also, since $P_M^{\mathrm{BGK}}(u, 0)$ is known to have a logarithmic singularity in its derivative at $u = 0$, the possibility of logarithmic corrections to the error estimates (1.7) cannot be excluded.

Our results for x_M and x_{Mr}, and hence for the effective boundary condition in (3.10), are pure numbers; in standard units they depend on γ only through the scale factor l. Thus, they could never have been determined perturbatively by the Chapman–Enskog method, which is formally an expansion in γ^{-1}, and physically a small-gradient expansion; as such it is bound to fail at the boundary, where, e.g., the gradient of the density is infinite in most cases.[18,20] A Chapman–Enskog-type derivation of the boundary condition by Chaturvedi and Agarwal[26] gave a result reducing to the simple approximation (3.7) for the stationary case without an external potential, independent of the details of the scattering mechanism at the wall, a result clearly at variance with our more accurate results. The correction terms in ref. 26 are relevant only for the nonstationary case, or in the presence of external potentials. They are again approximations, albeit reasonable ones, of a quality comparable to (3.7). In two recent papers by Menon and Sahni[27] and Menon[28] a rather different expansion is used; these authors also derive the expression (3.10) (x_{Mr} equals the average of u^2 for a solution of unit current[12]); they then determine the distribution function by iterating a Green's function equation in terms of the number of

Table V. The Boundary Layer Part of the Density Profile $-n_b(x) = \lvert n_M(x) - x - x_M \rvert$ for Dilute Impurities at a Wall That Absorbs All Impurities, As Calculated in the BGK Model[a]

x	0	$\frac{1}{2}\sqrt{2}$	$\sqrt{2}$	$\frac{3}{2}\sqrt{2}$	$2\sqrt{2}$
Present method	0.43$\underline{7}$	0.17$\underline{3}$	0.1$\underline{0}$	0.065*	0.043*
Exact[25]	0.435804	0.171224	0.100032	0.067230	0.046775

[a] The error is one unit in the underlined decimal place; an asterisk denotes that no reliable error estimate can be given.

encounters of the particle with the wall (real or virtual). This expansion can be expected to converge toward the right distribution function,[29] but it is completely different from the Chapman–Enskog expansion. We comment no further on the effects of potentials and nonstationarity, since those topics will be treated in detail in forthcoming papers.[20]

The models treated in Sections 4 and 5 with $\beta_w \neq \beta$ are not meant to be a realistic description of a medium in contact with a wall at a different temperature; the wall will of course exchange heat with the medium as well as with the Brownian particles, and there will be a kinetic boundary layer in the medium, too. However, when the mean free path for the medium molecules is small compared to the velocity persistence length of the Brownian particles, the latter will not see the detailed structure of the medium boundary layer, but merely a linear temperature gradient and a sudden temperature jump at the wall:

$$T(x) \simeq T_w[1-\alpha(x+x_T)] \qquad \text{for} \quad x>0 \tag{6.2}$$

with x_T the temperature jump length, a quantity analogous to the Milne length. Thus, one has to solve the boundary value problem for the Klein–Kramers equation in the presence of a temperature gradient in addition to the temperature jump. Such a problem was considered in a recent paper.[30] The equilibrium solution $\Psi_0(\mathbf{u}, x)$ and the current-carrying solution $\Psi_c(\mathbf{u}, x)$ can be constructed; for the boundary layer solutions at least a perturbation theory, with α as the perturbation parameter, appears feasible. In lowest order one is led to the (exactly solvable) case of Brownian motion with a constant drift.[3,4,23]

The problem of Brownian motion in the presence of a (partially) absorbing sphere serves as a model system for some situations of practical interest: the growth of a condensation nucleus in a carrier gas mixed with a supersaturated vapor, or the burning of a small fuel droplet (with, e.g., an oxidant as the diffusing species). A preliminary analysis of kinetic boundary layer effects for this problem showed[31] that the number of particles absorbed by a droplet of radius R per unit time in a medium with a concentration of Brownian particles $n(\infty)$ far away from the sphere can be written as

$$4\pi R^2 j_{\text{abs}} = 4\pi R^2[R + x_M(R)]^{-1}\, n(\infty) \tag{6.3}$$

where $x_M(R)$ is a curvature-dependent Milne length, approaching x_M for $R \to \infty$. We recently succeeded[14] in developing a perturbation theory in the curvature R^{-1} for the kinetic boundary layer around a sphere, and in particular for $x_M(R)$, and determined the first two correction terms using the techniques developed in the present paper.

APPENDIX

In this appendix we sketch the derivation of the profiles for $T_t(x)$ and $T_x(x)$. We start from the identities

$$u_x^2 = \tilde{\chi}_0(u_t)[\tilde{\phi}_0(u_x) + \tilde{\phi}_2(u_x)] \tag{A.1a}$$

$$\tfrac{1}{2}u_t^2 = \tilde{\phi}_0(u_x)[\tilde{\chi}_0(u_t) - \tilde{\chi}_1(u_t)] \tag{A.1b}$$

which follow directly from the definitions (2.11) and (4.9). Taking averages of these quantities in the albedo solution, as specified by (4.10), (4.19), and (4.20), and using the definitions (4.31) and (4.32) and the biorthonormality relations, gives

$$n_g^N(x)\, T_{xg}^N(x) = \sum_{n=0}^{N-1} \alpha_n^{Ng0} \exp(-\lambda_{n0}^N x)(c_{n00}^N + c_{n02}^N) = \alpha_0^{Ng0} \tag{A.2a}$$

$$n_g^N(x)\, T_{tg}^N(x) = \sum_{n=0}^{N-1} [\alpha_n^{Ng0} \exp(-\lambda_{n0}^N x) - \alpha_n^{Ng1} \exp(-\lambda_{n1}^N x)] \tag{A.2b}$$

In the first of these expressions we used the relation (2.14) for $m=1$, which ensures that $c_{n00}^N + c_{n02}^N$ vanishes whenever λ_{n0}^N is unequal to zero. For $n=0$ one of course has $c_{00m}^N = \delta_{m0}$. The temperature profiles are found from (A.2) by substituting the expression (4.24) for $n_g(x)$. This leads to

$$T_{xg}^N(x) = \frac{n_g^N(\infty)}{n_g^N(x)} = \frac{\alpha_0^{Ng0}}{\sum_n \alpha_n^{Ng0} \exp(-\lambda_{n0}^N x)} \tag{A.3a}$$

$$T_{tg}^N(x) = 1 - \frac{\sum_n \alpha_n^{Ng1} \exp(-\lambda_{n1}^N x)}{\sum_n \alpha_n^{Ng0} \exp(-\lambda_{n0}^N x)} \tag{A.3b}$$

One sees that the longest decay length in $T_{xg}^N(x)$ is $\lambda_{10}^N \simeq 1$, whereas the longest decay length in $T_{tg}^N(x)$ is $\lambda_{01}^N \simeq \sqrt{2}$; this discrepancy in decay lengths is also physically reasonable, as is discussed in the text after (4.26).

The solution (1.5) for the Milne problem can be written as $P_M(u_x, x)\, \chi_0(u_t)$, hence all α_n^{NMl} with $l \neq 0$ vanish. However, there are additional contributions from $x\phi_0(u_x)$ in the current contribution $\Psi_c(u_x, x)\, \chi_0(u_t)$. Thus, we have

$$n_M^N(x) \langle u_x^2 \rangle_M^N(x) = \alpha_0^{NM} + x \tag{A.4a}$$

$$n_M^N(x)\, T_{tM}^N(x) = n_M^N(x) \tag{A.4b}$$

To obtain $T_{tM}^N(x)$, we use (5.9) and (5.10) and obtain ($x_M^N = \alpha_0^{NM}$)

$$T_{xM}^N(x) = \frac{x + x_M^N}{n_M^N(x)} - \frac{1}{[n_M^N(x)]^2} \tag{A.5}$$

For a linear combination of Milne and albedo solutions of type (5.4), the transverse temperature is obtained from (5.8). For $T^N_{x\sigma}(x)$ one obtains by straightforward substitution

$$n^N_\sigma(x)\, T^N_{x\sigma}(x) = x_M + x + A_r \alpha_0^{Ng0} - [n^N_\sigma(x)]^{-1} \tag{A.6}$$

from which the profiles $T^N_{x\sigma}(x)$ shown in Fig. 6 follow immediately.

ACKNOWLEDGMENT

This work was supported in part by the Fonds zur Förderung der wissenschaftlichen Forschung in Österreich.

REFERENCES

1. S. Chapman and T. G. Cowling, *The Mathematical Theory of Non-Uniform Gases* (Cambridge University Press, Cambridge, 1970); J. M. Ferziger and H. G. Kaper, *Mathematical Theory of Transport Processes in Gases* (North-Holland, Amsterdam, 1972).
2. C. Cercignani, *Theory and Application of the Boltzmann Equation* (Scottish Academic Press, Edinburgh, 1975).
3. T. W. Marshall and E. J. Watson, *J. Phys. A* **18**:3531 (1985).
4. T. W. Marshall and E. J. Watson, *J. Phys. A* **20**:1345 (1987).
5. O. Klein, *Ark. Mat. Astron. Fys.* **16**(5):1 (1922).
6. H. A. Kramers, *Physica* **7**:284 (1940).
7. S. Waldenstrøm, K. Razi Naqvi, and K. I. Mork, *Ark. Fys. Semin. Trondheim*, No. 8 (1983); *Phys. Rev. A* **28**:1659 (1983).
8. H. Grad, *Commun. Pure Appl. Math.* **2**:325, 331 (1949).
9. R. E. Marshak, *Phys. Rev.* **71**:443 (1947).
10. K. Razi Naqvi, K. I. Mork, and S. Waldenstrøm, *Phys. Rev. Lett.* **49**:2710 (1983); K. I. Mork, K. Razi Naqvi, and S. Waldenstrøm, *J. Coll. Interf. Sci.* **98**:103 (1984); D. C. Sahni, *Phys. Rev. A* **30**:2056 (1984).
11. V. Kumar and S. V. G. Menon, *J. Chem. Phys.* **82**:917 (1985).
12. M. A. Burschka and U. M. Titulaer, *J. Stat. Phys.* **25**:569 (1981).
13. M. A. Burschka and U. M. Titulaer, *J. Stat. Phys.* **26**:59 (1981).
14. M. E. Widder and U. M. Titulaer, *Physica A* **154**:452 (1989).
15. U. M. Titulaer, *Physica A* **91**:321 (1978); **100**:234 (1980).
16. C. D. Pagani, *Boll. Un. Mat. Ital.* **3**(4):961 (1970).
17. R. Beals and V. Protopopescu, *J. Stat. Phys.* **32**:565 (1983).
18. U. M. Titulaer, *J. Stat. Phys.* **37**:589 (1984).
19. U. M. Titulaer, *Phys. Lett. A* **108**:19 (1985).
20. A. Kainz and U. M. Titulaer, to be published.
21. H. A. Bethe, M. E. Rose, and L. P. Smith, *Proc. Am. Phil. Soc.* **70**:573 (1983).
22. J. V. Selinger and U. M. Titulaer, *J. Stat. Phys.* **36**:293 (1981).
23. M. A. Burschka and U. M. Titulaer, *Physica A* **112**:315 (1982).
24. M. E. Widder, Diploma Thesis, Linz University, unpublished.

25. T. Ytrehus, I. I. Smolderen, and I. F. Wendt, *Phys. Fluids* **18**:1253 (1975).
26. S. Chaturvedi and G. S. Agarwal, *Z. Phys. B* **52**:247 (1983).
27. S. V. G. Menon and D. C. Sahni, *Phys. Rev. A* **32**:3832 (1985).
28. S. V. G. Menon, *Phys. Lett. A* **119**:210 (1986).
29. S. V. G. Menon, V. Kumar, and D. C. Sahni, *Physica A* **135**:63 (1986).
30. M. E. Widder and U. M. Titulaer, *J. Stat. Phys.* **55**:1109 (1989).
31. G. R. Kneller and U. M. Titulaer, *Physica A* **129**:514 (1985).